J. Micromech. Microeng. **22** (2012) 015011 (7pp) doi:10.1088/0960-1317/22/1/015011

The influences of transverse loads on electrothermal post-buckling microbeams

Xing Chen[1], LianSheng Ma[1,2], YingMei Zheng[1], Xinxin Li[3] and Dong-Weon Lee[1,4]

[1] MEMS and Nanotechnology Laboratory, School of Mechanical Systems Engineering, Chonnam National University, Gwangju, Republic of Korea
[2] School of Science, Lanzhou University of Technology, Lanzhou, People's Republic of China
[3] State Key Laboratory of Transducer Technology, and Science and Technology on Microsystem Laboratory, Shanghai Institute of Microsystem and Information Technology, Chinese Academy of Sciences, Shanghai, People's Republic of China

E-mail: mems@jnu.ac.kr

Received 6 July 2011, in final form 18 October 2011
Published 20 December 2011
Online at stacks.iop.org/JMM/22/015011

Abstract
We report on a nonlinear equation-based closed-form solution for a spring-loading-enclosed electrothermal post-buckling microbeam that expresses (a) the relation between the compressive loads and its corresponding lateral deflections and (b) the threshold loads required to trigger the buckling phenomenon, under the condition of a variety of transverse loads. Our theoretical research reveals that the post-buckling behavior varies considerably under different transverse load ranges. Three types of double-clamped microbeams connected to microsprings with different dimensions and compliances representing transverse loads were fabricated and measured using microelectromechanical systems (MEMS) technology. Excellent agreement was found between our theoretical analysis and experimental results to confirm our exact solutions. It proves that the influences on thermal post-buckling behavior are dependent on different microbeam dimensions and microspring compliances (i.e., transverse loads). Therefore, an electrothermal buckling/post-buckling beam under external transverse loads can be accurately predicted using our theoretical model, which can be applied to either existing microdevices that are based on similar principles or other potential applications.

(Some figures in this article are in colour only in the electronic version)

1. Introduction

Buckling and post-buckling research is mainly concerned with the instability of a structure subject to in-plane axially compressive loads. It is of importance to the safety of engineering structures for avoiding instability-induced failure [1]. Recently, just as important as its negative factor, buckling related research is increasingly beneficial to advancements of the tricky design and novel actuation mechanism in the micro-electromechanical system (MEMS). Described as a rapid transition between two stable states, snap-through buckling is suitable for many MEMS applications, including micromirrors [2], latch-lockers [3], micro-mechanical memory with on-chip readout [4], energy harvesting [5], microactuators [6–8], and microswitches [9, 10]. In addition, post-buckling, which is continuing loading behavior after buckling, has not only widely served to MEMS actuation, but also been fundamentally investigated by using MEMS devices as effective tools, e.g., electromechanical buckling has been experimentally validated with an electrostatic force driving clamped-guided beam [11]. Compared to electrostatic or electromagnetic actuation, electrothermal actuation is significantly dominant in this area, as it contributes to large output forces and large displacements that can more readily cause post-buckling behavior [12, 13]. Thus, study on electrothermal buckling and post-buckling behavior of microbeams has drawn considerable attention.

Most electrothermal buckling/post-buckling research has covered either theoretical analysis or experimental work.

[4] Author to whom any correspondence should be addressed.

They have reported that exact post-buckling solutions are prohibitively complex, because the related equations are highly nonlinear, involving the nonlinear bending moment–curvature relationship and/or nonlinear kinematic relations [14]. Consequently, even though both theoretical study and experimental realization is given in [15], their analysis on nonlinear buckled configuration of the beams is given in the form of an elliptic integral that is not easy to solve, hence exempting exact solutions. Recently, a closed-form expression for buckled configurations as a function of an applied axial load with different boundary conditions was well obtained using nonlinear post-buckling analysis [16]. However, their models are limited to a simple double-clamped beam only under uniaxial buckling load. Taking into account practical engineering cases, usually, post-buckling beams are synchronously subject to not only axial buckling load, but also counteractive transverse loads from the targeted object. Furthermore, considering buckling applications in MEMS actuation or resonance, which are the main objective herein as well as most related literature claims to be a research target, any external transverse load or impact exerted on the buckling beam is inevitable. In order to guide the design of practical electrothermal buckling-based MEMS applications, we present both theoretical and experimental methods for the post-buckling of a beam-like structure that simultaneously suffers from axial buckling loads and external transverse loads, and the influence of different transverse loads on post-buckling behavior.

2. Theoretical investigation for nonlinear buckling analysis

2.1. Structural model and exact solution based on analytical method

Thermal load-induced post-buckling of a beam-like structure subject to additional transverse loads is studied theoretically. The structure is modeled using large deflection theory, where double-clamped beams connected to springs with different spring compliances at the mid-span that represent various transverse loads are considered. Equations governing the axial and transverse deformations of the beams are derived. Two equations are reduced to a single nonlinear fourth-order integral-differential equation governing the transverse deformations. The nonlinear equation is directly solved without the use of approximation. Finally, a closed-form solution for thermal post-buckling deformation is obtained as a function of the applied thermal load.

Using the energy principle, the equilibrium equations and boundary conditions based on classical beam theory are derived in our previous works [17]. The closed-form solution for the buckled configuration of a beam with fixed–fixed boundary conditions is given,

$$W(x) = c\left\{1 - \frac{a}{\Gamma}X + \frac{1}{\Gamma}\sin(aX) - (1 - 2a^3\Lambda)\cos(aX)\right\}, \tag{1}$$

where $W(x)$ is the expression of deflections with respect to the axis x toward the centroidal axis of the beam, c is a constant related to the applied thermal load N, and is given by

$$c = \pm\frac{1}{\sqrt{f(a)}}\sqrt{\frac{N}{a^2} - 1}, \tag{2}$$

and

$$\Lambda = \frac{\beta}{\Gamma} \tag{3}$$

At the beginning stage of buckling, the configuration of a buckled beam is sufficiently close to the beam's initial straight configuration. In this case, the thermal load N at that instant of time is the critical buckling thermal load N_{cr}. The critical buckling load N_{cr} is obtained by letting $c = 0$: $N_{cr} = a^2_{min}$.

2.2. Buckling expression and the influence of different spring compliances on post-buckling behavior

The exact solution expressing deflection at the center of the beam $W(0)$, which is more explicit than the work in [17], can be further derived from equation (1) as follows:

$$W(0) = \pm\frac{2a^3\beta}{\Gamma\sqrt{f(a)}}\sqrt{\frac{N}{a^2} - 1}. \tag{4}$$

and the function $f(a)$ is given by

$$f(a) = \frac{1}{4a\Gamma^2\sin^2\frac{a}{2}} \times\left[2a + 2a\sin^2\frac{a}{2} - 2a\cos\frac{a}{2} - 12\sin\frac{a}{2}\left(1 - \cos\frac{a}{2}\right)\right], \tag{5}$$

and

$$\Gamma = \frac{1 - \cos\frac{a}{2}}{\sin\frac{a}{2}} + 2\beta a^3. \tag{6}$$

The characteristic equation for a beam with fixed–fixed boundary conditions is given by

$$2 - 2\cos\frac{a}{2} - \frac{a}{2}\sin\frac{a}{2} + 2\beta a^3\sin\frac{a}{2} = 0. \tag{7}$$

In the above equations, to generalize the subsequent results, we used the following non-dimensional variables:

$$X = \frac{x}{l}, \quad W = w\sqrt{\frac{A_x}{D_x}}, \quad N = \frac{N^T l^2}{D_x}, \quad \text{and} \quad \beta = \frac{D_x}{kl^3},$$

where β represents the dimensionless spring compliance.

Equation (2) shows the behavior of a post-buckling beam under different assumed transverse loads that are represented by a mechanical spring system, and the resulting deflection as a function of applied thermal axial driving loads is clearly described. Moreover, it demonstrates the variation of the dimensionless critical thermal buckling load N_{cr} (the point where $W(0)$ is equal to zero) with different values of dimensionless spring compliance β. This signifies that as our defined spring compliance β (i.e., the inverse of the transverse load) increases, N_{cr} required for buckling decreases up to that of the beam without a spring (i.e., no transverse load).

In addition, N_{cr} is a monotonically decreasing nonlinear function of β as demonstrated in figure 1 of [17]. N_{cr} turns

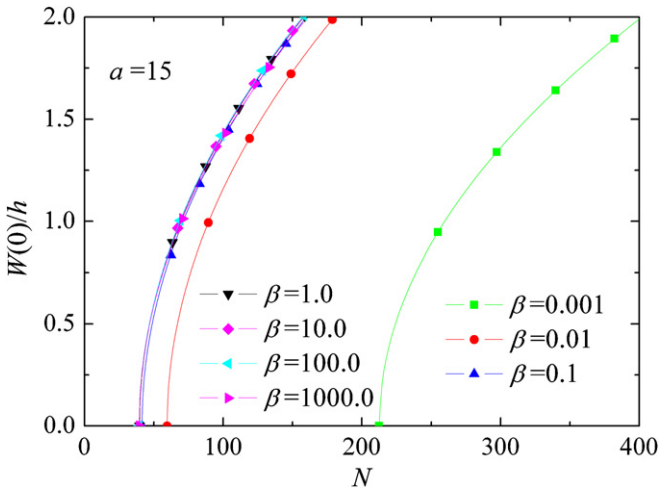

Figure 1. Influence on post-buckling behavior by variation of dimensionless spring compliance β, including dimensionless mid-span deflection $W(0)/h$ and the dimensionless critical thermal buckling load N_{cr}.

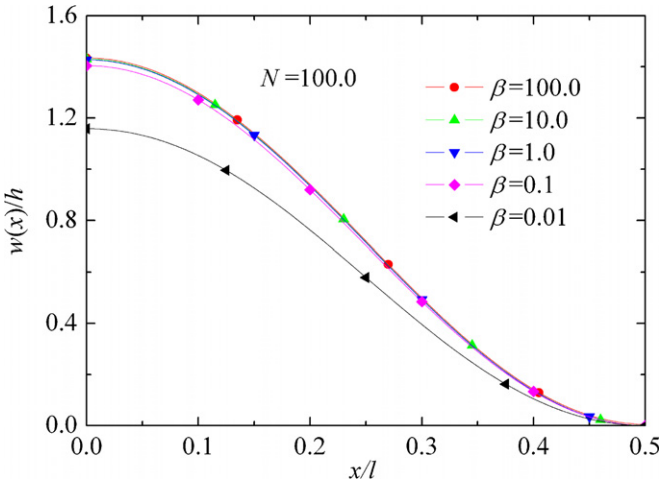

Figure 2. Deflection shape along the beam expressed as $W(x)/h$ with a variety of transverse spring compliances β under certain thermal buckling load.

out to be infinite when β approaches zero, while there is an obvious rapid decrease of N_{cr} with increase in β, and N_{cr} reaches a stable value when β exceeds a high value until infinity. In other words, the influence of spring compliance on thermal buckling behavior is obvious only for a small value range of β (i.e., a large stiffness k or large transverse load). In contrast, when the spring compliance β increases to high values, the effect on the critical thermal buckling load N_{cr} and the deflection at the center of the beam $W(0)$ becomes very small. This relationship involving three parameters can be clearly expressed from the previous equilibrium equation and boundary conditions, consisting of deflections at the midspan of the beam, axially compressive loads and various spring compliances. Figure 1 shows that N_{cr} decreases dramatically from β at 0.001 to 0.01. When β increases to a higher value in the range between 1 and 1000 or even higher values, the influence on post-buckling behavior seems to be insensitive to variations of β. Furthermore, equation (2) gives an expression for the deflection shape along the beam with a variety of transverse spring compliances, as shown in figure 2. It demonstrates the same phenomenon as that described in figure 1 that the degree of effect on post-buckling behavior differs from between small spring compliance and that at high value range.

Compared to previous theoretical works guided by the use of finite element analysis [18, 19] or analytical approximate solutions [15, 20] either in the form of an elliptic integral that is not easy to solve or involving approximation, the theoretical results reported in this study can be directly solved without approximation. A closed-form solution for thermal post-buckling deformation with high accuracy was obtained. As a result, our analytical method provides a simple and efficient solution for expressing post-buckling behavior of a microbeam or beam-like structures suffering from various transverse loads.

3. Experimental results

3.1. Fabrication process

Our experimental validation for the theoretical prediction investigated in this paper demonstrates not only the accuracy of our analytical solution, but also the feasibility to study the classical mechanics problem with single-crystal-structural devices at the microscale. Our testing system is based on micro-fabricated single-crystal-silicon (SCS) devices. SCS is a pure material with few mechanical defects, low residual stress and a large elastic deformation range. More importantly, compared to the conventional experimental methods [21, 22], micro-fabricated devices and MEMS technology can provide unique experimental testing conditions, behaving almost the same as the studied mathematical model; they have already been shown to be good tools for the investigation of fundamental mechanics and physics [23].

Double-clamped microbeams connected to microsprings were fabricated using a bulk micromachining process on a silicon-on-insulator (SOI) wafer with a 5 μm thick and 0.025 Ω cm highly-doped top device silicon layer. After standard cleaning (figure 3(*a*)), photolithography was performed on the front side to pattern the microstructures. The patterns were well aligned with the ⟨1 1 0⟩ crystal direction to confine an exact Young's modulus due to the anisotropic elasticity of silicon [24]. Then, deep reactive ion etching (DRIE) was used to etch the top silicon layer up to the buried oxide (BOX) (figure 3(*b*)). The fabricated structures demonstrate the desired vertically-shaped cross section of the beams as shown in figure 4. Finally, the structures were released in our lab-made hydrofluoric acid (HF) vapor etching system to prevent them from stiction with the substrate, due to surface capillary force (figure 3(*c*)). The fabricated microdevices were confirmed by both optical microscopy and scanning electron microscopy (SEM). Due to precise microfabrication, they were consistent with the ideal model, as illustrated in figure 4.

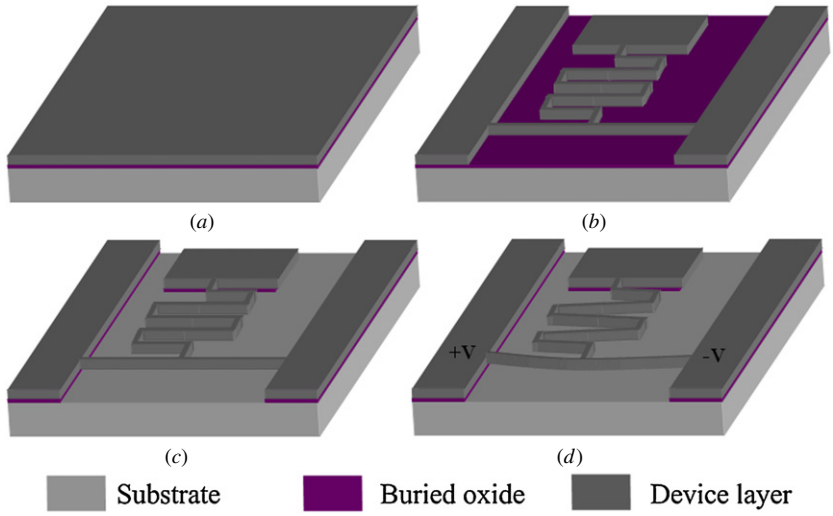

Figure 3. Main fabrication process on SOI wafer for the microdevices, and the schematic of post-buckling actuation principle.

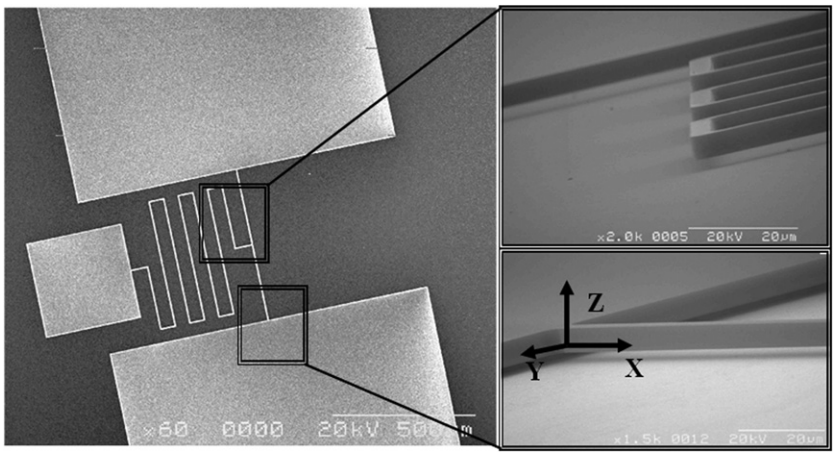

Figure 4. SEM images of fabricated double-clamped microbeam with microspring, and close-up of side view to show mechanical boundary conditions and suspended structure that is oriented by Cartesian coordinate system (*x, y, z*) with the origin at the middle of the beam (the origin in the figure is located at the end of the beam for legible vision, rather than the actual definition in our model).

3.2. Post-buckling generation and measurement

A group of microdevices with various dimensions and different transverse spring compliances were fabricated: $480 \times 4 \times 5\ \mu m^3$ with $k = 1.69\ N\ m^{-1}$ and $\beta = 0.024$; $480 \times 4 \times 5\ \mu m^3$ with $k = 0.056\ N\ m^{-1}$ and $\beta = 0.072$; and $560 \times 4 \times 5\ \mu m^3$ with $k = 1.69\ N\ m^{-1}$ and $\beta = 0.015$. When current flows through the electrodes, heat was induced throughout the microbeams due to an electro-thermal phenomenon. The increasing heat produced thermal strain as a result of the thermal-elastic effect. An optical microscope equipped with a charge-coupled device (CCD) camera and an image processing program was used to observe the deflection and capture image data. The input current was started at an extremely low value and adjusted gradually to a high value for the observation of the entire post-buckling process.

Initially, the double-clamped microbeams and microspring were undeformed, until the continuously increased current reached a critical point where sufficient compressive stress triggered buckling and subsequent post-buckling behavior, as shown in figure 3(*d*). Beyond this critical point, the microbeams and microsprings deformed further with higher input power, as shown in figure 5. A source meter (2400 series, Keithley Instruments, Inc., USA) was used to supply the current and record the feedback voltage; therefore, we could characterize the corresponding deflection as a result of power consumption. The self-buckling beams eased the centric load relative to the neutral surface, and provided good boundary conditions and a well-controlled electro-thermal load.

3.3. Results and discussion

In this experiment, to reduce errors, three types of microdevices with different dimensions and microsprings were measured using multiple samples. Each sample was tested repeatedly at least three times, using the same process. The average data were extracted from all samples and processes. Electrothermal post-buckling phenomenon is described as a multiphysics problem, coupled with electrothermal and thermal-elastic effects [25]. Electrothermal analysis has been

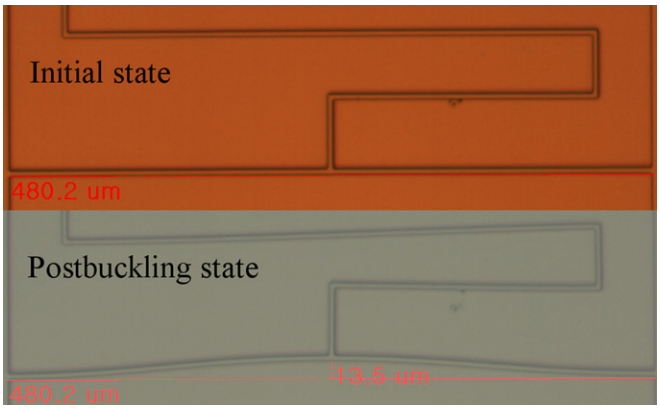

Figure 5. Optical images of double-clamped microbeam deflection and microspring deformation under post-buckling.

widely studied and well established [15, 26]; thus, our research did not involve and repeat this analytical work. Based on previous research, the average steady temperature as a function of input power can be readily calculated for use in our analysis. It is helpful to simplify the problem into a single thermal-elastic model, the theory of which is described in section 2. The maximum average temperature along the microbeams was kept around 700 °C to prevent any failure or recrystallization. In addition, in the range of the actuation temperature, contrary to the results reported in [27], no obvious plastic deformation occurred in the SCS microstructure. In terms of the tested micro-fabricated samples, the factors from residual stresses of the multilayers or variations of the cross section of the beam can be ignored [28–30], attributual to the SCS structural devices and a well-controlled fabrication technique.

Figure 6 shows the comparison between theoretical prediction and experimental results for deflections from three types of microdevices versus the average temperature calculated from input power, referred to the research [15]. The experimental results are all highly consistent with the predictions using the theoretical model. Unfortunately, our measurement method cannot determine the value of the critical point of buckling—the point at which the threshold of deflection occurs. The slight disagreement between our experimental and analytical results mainly occurs at the small deflection area and low temperature. One reason results from the difficulty in characterizing small deflections measured by an optical microscopy with 10% inaccuracy, due to its limited resolution. In the large deflection range, the output is much greater compared to the errors, so as to give higher consistent results. Another reasonable explanation is that we ignore the deformation of two ends of a double-clamped beam which are supported by elastic foundation in real devices rather than built-in conditions considered in our theoretical model. A similar phenomenon was observed and discussed in detail to explain the influence of substrate compliance in an associated problem [31–33].

To evaluate the predicted phenomenon demonstrated theoretically in section 2 that the degree of influence on thermal post-buckling behavior varies by value range of spring compliance, three types of micro-device configurations

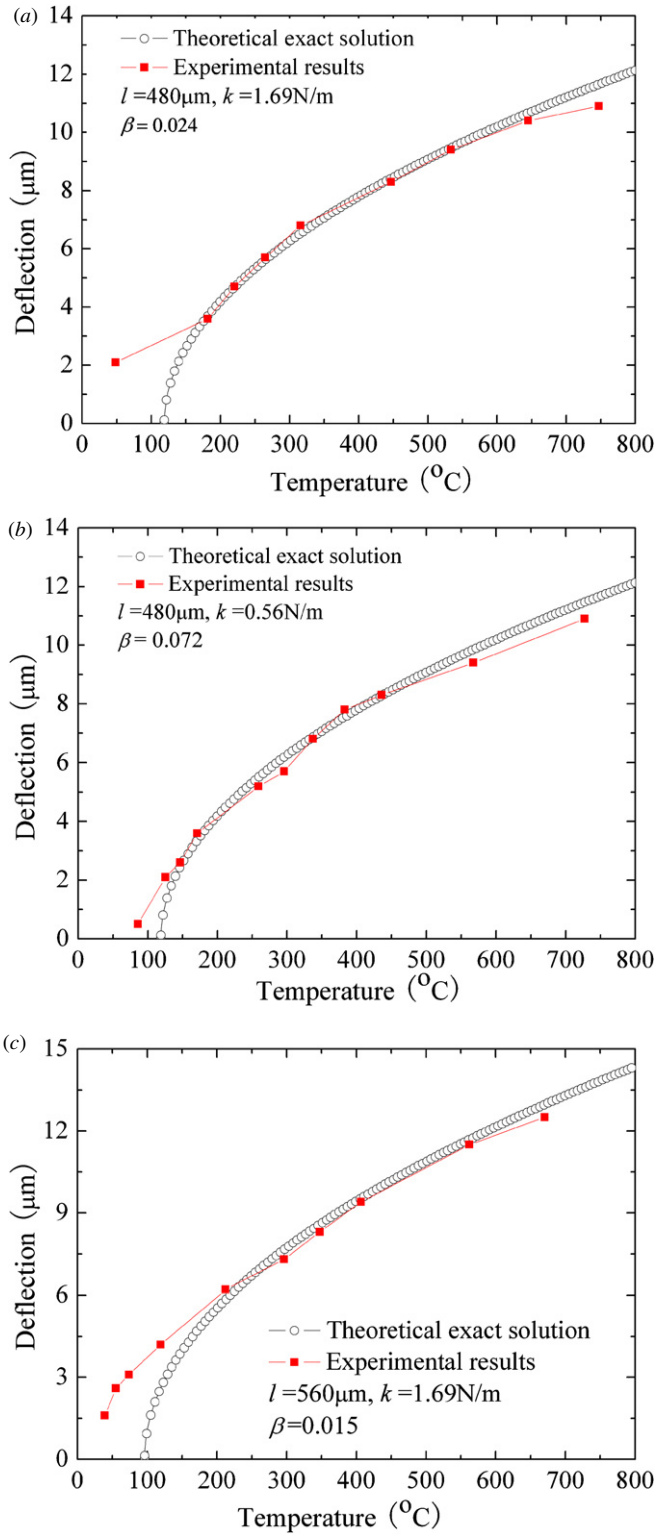

Figure 6. Plot of comparison between theoretical and experimental deflections versus average temperature for three types of microdevices.

with various spring compliances and dimensions have been tested, each pair of them share one property in common, i.e., either dimensions or spring compliance. First, the results from the microdevice shown in figure 6(*a*) are compared to that in figure 6(*c*), as both of them have the same spring

compliance. It is found that the two types of microdevices show somewhat different results, which is mainly caused by different microbeam dimensions.

Then, the two types of microdevices with identical dimensions but different spring compliances (i.e., $\beta = 0.024$ and $\beta = 0.072$, respectively) are compared, as shown in figures 6(*a*) and (*b*). They show different but close results, because their different values of β fall into a range in which the slope between N_{cr} and β is smooth, which is the same as we have predicted in the theoretical part. Therefore, the influence from their different compliances on post-buckling behavior exists, but is not significant. We note that even though post-buckling behavior is both experimentally and theoretically proved to be insensitive to variations of the spring compliances in this value range, through the comparison to the microbeams without spring in [17], which means that the spring compliance is infinite ($\beta = \infty$), an obvious difference is observed between the spring- and springless microdevices. It means that the spring representing transverse load more or less affects the buckling behavior, while the degree of influence on post-buckling behavior is decided by the value range of spring compliances. This finding agrees with the prediction based on our theory.

Our current research only provides experimental data for microdevices within a certain range of spring compliances, and does not include extremely stiff or soft springs. Very high stiffness may lead to a huge critical thermal buckling load and a relatively small deflection that will makes an accurate measurement more difficult. It is also not easy to fabricate an excessively soft spring constructed with very narrow and long beams. The extremely soft spring case can be assumed to be springless, which has been previously analyzed. Due to the rich information and data covered in our theoretical model, it is impossible to realize all the associated experimental work in this research. Since the validity of our theoretical model has been confirmed, more useful data included in our model will be exploited by other researchers for their specific applications. This research suggests that post-buckling microactuation behaves nonlinearly along with counteractive transverse loads. Buckling-based microactuation should be controlled within a proper range of actuation forces; otherwise, input power will nonlinearly increase with the required transverse force in the high value range. The understanding of the deformation of microspring is also useful to reveal the condition of potential energy stored in the spring system, which could help the frequency-tuning research [5, 23]. Our work provides an easy and comprehensive method to aid the design of similarly configured structures [34, 35].

4. Conclusion

With the broad incorporation of buckling and post-buckling mechanisms into MEMS applications, it is important to understand buckling/post-buckling behavior in practical microdevices.

We have investigated post-buckling behavior of single-crystal-silicon (SCS) double-clamped microbeams under various transverse loads that were represented by different microsprings. A nonlinear equation was directly solved without the use of approximation, and a closed-form solution for thermal post-buckling deformation was obtained as a function of the applied thermal load. A more explicit exact solution expressing deflection at the center of the beam was derived. The influence of post-buckling behavior under different values of spring compliance can be accurately predicted by the theoretical model, including the critical thermal buckling load, the deflection at the center of the beam, and the deflection shape along the beam. Interestingly, our theoretical model indicates that the effect on thermal post-buckling behavior varies distinctly with the value range of spring compliance. SCS microdevices based on IC technology were fabricated using a microfabrication method with similar boundary conditions, just like those described in the theoretical model. We found that the experimental results were highly consistent with the predictions from the proposed theoretical model, and that the consistency is higher than results from other research, due to the exact solutions in the theoretical model and well-fabricated microsamples. The theoretical prediction that the influence on thermal post-buckling behavior varies by different spring compliances was validated based on three sample configurations. This study is of theoretical and practical significance to investigate the fundamental physics, and guide the design and optimization of novel and more complex MEMS devices.

Acknowledgment

This work was supported by the Ministry of Knowledge Economy of the Korean government, and by the World Class University (WCU) project (R32-2009-000-20087-0), Republic of Korea. Professor LianSheng Ma personally thanks the NNSF of China(11072100).

References

[1] Vaidya A S, Vaidya U K and Uddin N 2008 Impact response of three-dimensional multifunctional sandwich composite *Mater. Sci. Eng.* A **472** 52–8

[2] Quevy E, Bigotte P, Collard D and Buchaillot L 2002 Large stroke actuation of continuous membrane for adaptive optics by 3D self-assembled microplates *Sensors Actuators* A **95** 183–95

[3] Chen W C, Lee C K, Wu C Y and Fang W L 2005 A new latched 2×2 optical switch using bi-directional movable electrothermal H-beam actuators *Sensors Actuators* A **123–124** 563–9

[4] Roodenburg D, Spronck J W, van der Zant H S J and Venstra W J 2009 Buckling beam micromechanical memory with on-chip readout *Appl. Phys. Lett.* **94** 183501

[5] Jung S M and Yun K S 2010 Energy-harvesting device with mechanical frequency-up conversion mechanism for increase power efficiency and wideband operation *Appl. Phys. Lett.* **96** 11906

[6] Ko J S, Lee M L, Lee D S, Choi C A and Kim Y T 2002 A laterally-driven bistable electromagnetic microrelay *Appl. Phys. Lett.* **81** 547–9

[7] Han J S, Ko J S, Kim Y T and Kwak B M 2002 Parametric study and optimization of a micro-optical switch with a laterally driven electromagnetic microactuator *J. Micromech. Microeng.* **12** 939–47

[8] Gerson Y, Krylov S and Ilic B 2010 Electrothermal bistability tuning in a large displacement micro actuator *J. Micromech. Microeng.* **20** 112001
[9] Han J S, Ko J S and Korvink J G 2004 Structural optimization of a large-displacement electromagnetic Lorentz force microactuator for optical switching applications *J. Micromech. Microeng.* **14** 1585–96
[10] Eun Y k, Na H J, Jeong B W, Lee J I and Kim J B 2009 Bidirectional electrothermal electromagnetic torsional microactuators for large angular motion at dc mode and high frequency resonance mode operation *J. Micromech. Microeng.* **19** 065023
[11] Salih S A and Elata D 2006 Experimental validation of electromechanical buckling *J. Microelectromech. Syst.* **15** 1656–62
[12] Cao A, Kim J B and Lin L W 2007 Bi-directional electrothermal electromagnetic actuators *J. Micromech. Microeng.* **17** 975–82
[13] Lin L W and Lin S H 1998 Vertically driven microactuators by electrothermal buckling effects *Sensors Actuators* A **71** 35–9
[14] Ioannidis G, Mahrenholtz O and Kounadis A N 1993 Lateral post-buckling analysis of beams *Arch. Appl. Mech.* **63** 151–8
[15] Chiao M and Lin L W 2000 Self-buckling of micromachined beams under resistive heating *J. Microelectromech. Syst.* **9** 146–51
[16] Nayfeh A H and Emam S A 2008 Exact solution and stability of postbuckling configurations of beams *Nonlinear Dynam.* **54** 395–408
[17] Chen X, Ma L S, Zheng Y M and Lee D W 2011 Theoretical analysis of postbuckling behavior with experimental validation using electrothermal microbeams *Appl. Phys. Lett.* **98** 073107
[18] Michael A and Kwok C Y 2007 Buckling shape of elastically constrained multi-layered micro-bridges *Sensors Actuators* A **135** 870–80
[19] Shamshirsaz M and Asgari M B 2008 Polysilicon micro beams buckling with temperature-dependent properties *Microsyst. Technol.* **14** 957–61
[20] Lindberg U, Soderkvist J, Lammerink T and Elwenspoek M 1993 Quasi-buckling of micromachined beams *J. Micromech. Microeng.* **3** 183–6
[21] Simitses G J 1986 Buckling and postbuckling of imperfect cylindrical shells: a review *Appl. Mech. Rev.* **39** 1517–24
[22] Królak M and Młotkowski A 1996 Experimental analysis of post-buckling and collapse behaviour of thin-walled box-section beam *Thin Walled Struct.* **26** 287–314
[23] Sarif M T A 2000 On a tunable bistable MEMS-theory and experiment *J. Microelectromech. Syst.* **9** 157–70
[24] Hopcroft M A, Nix W D and Kenny T W 2010 What is the Young's modulus of silicon *J. Microelectromech. Syst.* **19** 229–38
[25] Riethmuller W and Benecke W 1988 Thermally excited silicon microactuators *IEEE Trans. Electron Devices.* **35** 758–63
[26] Lin L W and Chiao M 1996 Electrothermal responses of lineshape microstructures *Sensors Actuators* A **55** 35–41
[27] Yang E H and Fujita H 1999 Reshaping of single-crystal silicon microstructures *Japan. J. Appl. Phys.* **38** 1580–3
[28] Saif M T A and MacDonald N C 1998 Measurement of forces and spring constants of microinstruments *Rev. Sci. Instrum.* **69** 1410–22
[29] Park S H and Hah D Y 2008 Pre-shaped buckled-beam actuators: theory and experiments *Sensors Actuators* A **148** 186–92
[30] Carr S M and Wybourne M N 2003 Elastic instability of nanomechanical beams *Appl. Phys. Lett.* **82** 709–11
[31] Zhao M H, Yang F and Zhang T Y 2007 Delamination buckling in the microwedge indentation of a thin film on an elastically deformable substrate *Mech. Mater.* **39** 881–92
[32] Zhao T Y, Su Y J, Qian C F, Zhao M H and Chen L Q 2000 Microbridge testing of silicon nitride thin films deposited on silicon wafers *Acta Mater.* **48** 2843–57
[33] Yu H H and Hutchinson J W 2002 Influence of substrate compliance on buckling delamination of thin films *Int. J. Fract.* **113** 39–55
[34] McCarthy M, Tiliakos N, Modi V and Frechette L G 2007 Thermal buckling of eccentric microfabricated nickel beams as temperature regulated nonlinear actuators for flow control *Sensorors Actuators* A **134** 37–46
[35] Cao A, Yuen P and Lin L W 2007 Microrelays with bidirectional electrothermal electromagnetic actuators and liquid metal wetted contacts *J. Microelectromech. Syst.* **16** 700–8